

Phenomenology Tools on Cloud Infrastructures using OpenStack

I. CAMPOS^{1*}, E. FERNÁNDEZ-DEL-CASTILLO^{1†}, S. HEINEMEYER^{1‡},
A. LOPEZ-GARCIA^{1§}, F. V.D. PAHLEN^{1,2¶} AND G. BORGES^{3**}

¹ Instituto de Física de Cantabria (CSIC-UC), E-39005 Santander, Spain

² Instituto de Biocomputacion y Fisica de Sistemas Complejos - BIFI
University of Zaragoza, E-50200, Zaragoza, Spain

³ Laboratorio de Instrumentacao e Fisica Experimental de Particulas - LIP
PT-1000-149 Lisboa, Portugal

Abstract

We present a new environment for computations in particle physics phenomenology employing recent developments in cloud computing. On this environment users can create and manage “virtual” machines on which the phenomenology codes/tools can be deployed easily in an automated way. We analyze the performance of this environment based on “virtual” machines versus the utilization of physical hardware. In this way we provide a qualitative result for the influence of the host operating system on the performance of a representative set of applications for phenomenology calculations.

* email: isabel.campos@csic.es

† email: enolfc@ifca.unican.es

‡ email: Sven.Heinemeyer@cern.ch

§ email: aloga@ifca.unican.es

¶ email: pahlen@ifca.unican.es

|| MultiDark Fellow

** email: goncalo@lip.pt

1 Introduction

Particle physics is one of the main driving forces in the development of computing and data distribution tools for advanced users. Nowadays computations in particle physics phenomenology take place in a diversified software ecosystem. In a broad sense we can speak in terms of two different categories: commercial or proprietary software, and software developed by the scientific collaborations themselves.

Commercial software is distributed under the terms of a particular end-user license agreement, which defines how and under which circumstances the software should be deployed and used. In the field of particle physics phenomenology such agreements are undertaken by the scientific institutions, which afterwards offer this software as a service to their researchers. This is the case of the most common software packages employed in the area, such as **Mathematica**, **Matlab**, etc.

Scientific collaborations develop also their own software, often in open source mode under a copy/left license model. In this way researchers can download this software, use it as it is, or implement modifications to better solve their particular analysis following a GNU General Public License style¹.

From a technical point of view, most of the codes are developed on Fortran or C/C++. They become very modular, because typically they are the result of the work of a collaborative team on which each member is in charge of a particular aspect of the calculation. Software packages evolve with the necessity of analyzing new data, simulating new scenarios at present and future colliders. The evolution implies the inclusion of new modules, or functions, which call and interconnect other modules in the code, and/or make external calls to proprietary software like **Mathematica** to perform basic calculations.

The knowledge of the collaboration and the basics of the physics approach often resides in the core parts of the code, which remain almost unaltered for years, while the development of the software package takes place to include new features. The core of the software package acts like a sort of legacy code. The inclusion of new modules to the software package needs to be done in such a way that these legacy parts remain untouched as much as possible, because its modification would affect all modules already present in ways sometimes very difficult to disentangle, or to predict. All this reflects in difficulties when it comes to compile those codes together with more modern ones. Often there are issues with compilers which cannot be easily solved and require a very deep insight in the code to be able to install it.

Some of the codes developed in the framework of scientific collaborations are not open-source, and therefore the sources are closed to external researchers. This reflects situations of competitiveness between groups, and the fact that the knowledge of the group often resides in the developed code, and therefore needs to be protected due to Intellectual Property Rights (IPR).

In such situations only the executable binaries are made externally available by the collaboration, which poses limitations on the architecture and operating systems, library versions, etc. on which the codes can be executed.

A further level of integration arises when one needs to deal with complex workflows. This is a most common scenario in particle physics phenomenology computations: each step of

¹See http://www.gnu.org/software/gsl/manual/html_node/GNU-General-Public-License.html for more details

the calculation requires as input the output of the previous code in the workflow. Therefore, the installation of several software packages is unavoidable nowadays when, for instance, the work concerns simulation, prediction or analysis of LHC data/phenomenology. The installation of several of those software packages on the same machine is often not trivial since one needs to install potentially conflicting software on the same machine: different libraries for each of these software packages, sometimes even different compiler versions, etc.

The scenario described results in practical difficulties for researchers, which translate into time consuming efforts for software deployment, up to impossibility of deployment due to software or architecture restrictions.

There is a general agreement in the community that setting up a proper computing environment is becoming a serious overhead for the everyday work of researchers. It is often the case that they need to deploy locally in their clusters (or even on their own desktops) all the software packages required for the calculations, each of them with their particular idiosyncrasies regarding compiler versions, dynamic libraries, etc. In this case the intervention of cluster system managers is also not of much help because a generic cluster cannot accommodate so many options without disturbing the work of everyone, or generating an unsustainable work overhead to the system administrator.

The main idea of this work is to exploit the flexibility of operating system virtualization techniques to overcome the problems described above. We will demonstrate how the already available solutions to deploy cloud computing services [1] can simplify the life of researchers doing phenomenology calculations and compare the performance to “more traditional” installations.

As will be shown along the article, one obvious solution where virtualization can help with the problems described above is the deployment of tailored virtual machines fitting exactly the requirements of the software to be deployed. This is specially the case when one deals with deploying pre-compiled binaries. However, the work described here aims for a more complete solution going from user authentication and authorization, to automation of code installation and performance analysis.

We want to remark that virtualization techniques are already widely used in most centres involved in the European Grid Initiative [2] as a fault-tolerant mechanism that simultaneously allows to simplify the maintenance and operation of the main grid services. However, those services remain static from the end users perspective, with little or no possibility to change, tune or enhance the execution environments. This work is motivated by the necessity of exploring a more efficient use of computing resources also at the level of the end user. For this purpose, we are exploring ways in which a Cloud service could be offered as an alternative to experienced users for which grid infrastructures are no longer able to satisfy their requirements. A mechanism for authentication and authorization based on VOMS [3] has been developed and integrated in our user service provision model to allow interoperability and a smooth, transparent transition between grid and IAAS cloud infrastructures.

Code performance using virtualized resources versus performances on non-virtualized hardware is also a subject of debate. Therefore it is interesting to make an efficiency analysis for real use cases, including self-developed codes and commercial software in order to shed some light on the influence on the performance of the host operating system on virtualized environments.

The hardware employed for all the tests described in the article is a server with 16GB

of RAM (well above the demand of the applications) with four Intel Xeon Processors of the family E3-1260L, 8M of Cache and running at 2,40GHz. In order to have a meaningful evaluation, we have disabled the power efficiency settings in the BIOS to have the processors running at maximum constant speed. We have also disabled the Turbo boost features in the BIOS because it increases the frequency of the individual cores depending on the occupancy of the cores, therefore distorting our measures. For the sake of completeness we have evaluated as well the influence of enabling the Hyperthreading features of the individual cores to demonstrate how virtualization and Hyperthreading together influence the performance of the codes.

The layout of the article is as follows. In Section 2 we describe the architecture and implementation of the proposed solutions; Sections 3 and 4 analyze two different real use cases, together with the respective performance evaluations. The first case focuses on the effects of the “virtual” environment on single process runs, whereas the second case deals with the potential speed-up via MPI parallelization on virtualized hardware. The last section contains our conclusions. The very technical details about authentication and user authorization as well as detailed numbers about our comparisons can be found in the Appendix.

2 Cloud Testbed and Services

2.1 OpenStack deployment

The deployment of cloud computing services requires the installation of a middleware on top of the operating system (Linux in our case), that enables the secure and efficient provision of virtualized resources in a computing infrastructure. There are several open-source middleware packages available to build clouds, with OpenNebula [4] and OpenStack [5] being the most used in the scientific data-centers of the European Grid Infrastructure.

After an evaluation of both OpenNebula and OpenStack, we have chosen the latter as middleware for our deployment due to its good support for our hardware and its modular architecture, which allows it to add new services without disrupting the already existing ones, and to scale easily by replicating services. OpenStack has a developer community behind that includes over 180 contributing companies and over 6,000 individual members and its being used in production infrastructures like the public cloud at RackSpace². Being written in Python is also an advantage since we can profit from our expertise in the language to solve problems and extend the features of the system.

OpenStack is designed as a set of inter-operable services that provide on-demand resources through public APIs. Our OpenStack deployment, based on the Essex release (fifth version of OpenStack, released on April 2012), has the following services, see Fig. 1:

- Keystone (identity service), provides authentication and access control mechanisms for the rest of components of OpenStack.
- Nova (compute service) manages virtual machines and their associated permanent disks (Volumes in OpenStack terminology). The service provides an API to start and stop virtual machines at the physical nodes; to assign them IP addresses for network

²See <http://www.rackspace.com/cloud/>.

connectivity; and to create snapshots of running instances that get saved in the Volume area. The volumes can also be used as a pluggable disk space to any running virtual machine.

- Glance (image management service) provides a catalog and repository for virtual disk images, which are run by Nova on the physical nodes.
- Horizon, a web-based dashboard that provides a graphical interface to interact with the services.

OpenStack provides also a object storage service but it's not currently used in our deployment.

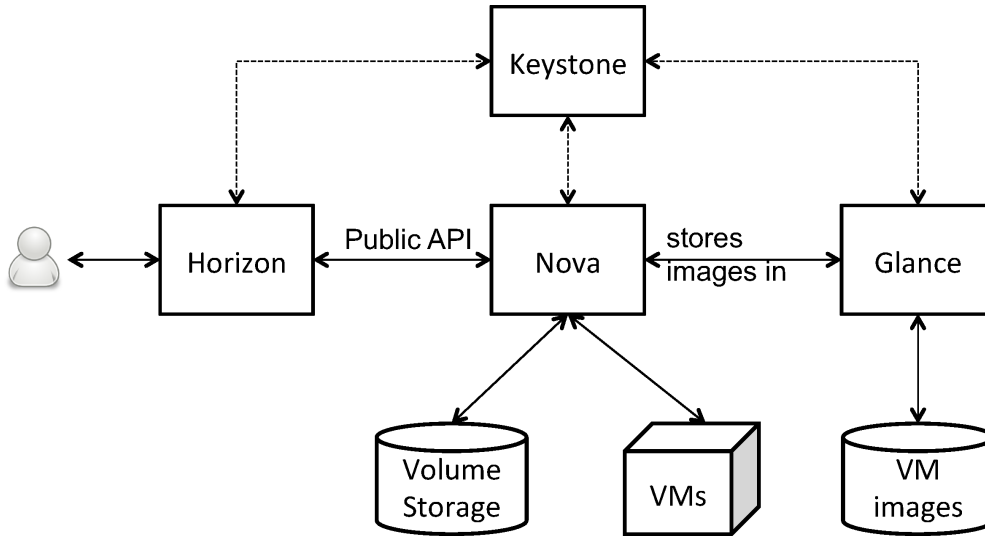


Figure 1: OpenStack deployment. Keystone provides authentication for all the services; Nova provides provisioning of virtual machines and associated storage; Glance manages the virtual machine images used by Nova; Horizon provides web-based interface built on top of the public APIs of the services.

Our Nova deployment provides virtual machines using 16 servers as described in the introduction running Linux with Xen [6] 4.0.1 as hypervisor. Volume storage for the virtual machines is provided using two identical servers with a quad-core Intel Xeon E5606 CPU running at 2.13GHz with 3GB of RAM, 4 TB of raw disk and two 1Gb Ethernet. Glance runs on a server with similar hardware.

Users of the infrastructure start virtual machines by selecting one image from the Glance catalog and the appropriate size (i.e. number of cores, amount of RAM and disk space) for their computing needs. The available sizes are designed to fit the physical machine with a maximum of 8 cores and 14GB of RAM (2GB of RAM are reserved for the physical machine Operating System, Xen hypervisor and OpenStack services) per machine.

The use of an open-source software allows us to adapt the services to better suit the needs of a scientific computing environment: we have expanded the authentication of Keystone to support VOMS and LDAP-based identities as shown in Appendix A and we have developed an image contextualization service with a web interface built on top of Horizon.

2.2 Image Contextualization

In an infrastructure as a service cloud, users become the administrators of their machines. Instead of submitting jobs with their workload to a batch system where the software is previously configured, they are provided with virtual machines with no extra help from the resource provider. The installation and configuration of any additional software must be performed by the final users. This provides users with flexibility to create tailored environments for running their software, but requires them to perform tedious administrative operations that are prone to errors and not of interest for most users.

This problem has been partially solved by the CernVM File System [7] —developed to deploy High Energy Physics software on distributed computing infrastructures— that provides a read-only file system for software. However, its centralized design renders it unpractical for software that changes frequently or is still being developed; it is also limited to software distribution, which may not be enough for having a working environment for the researchers. We have developed an image contextualization service that frees the user from downloading, configuring and installing the software required for their computations when the virtual machine is instantiated. This kind of approach does not only provide software installation, but also allows to customize every other aspect of the machine configuration, e.g. adding users, mount file-systems (even the CernVM File System) and starting services.

The service has three main components: an application catalog that lists all the available applications; a contextualizer that orchestrates the whole process and takes care of application dependencies; and a set of installation scripts that are executed for installation and configuration of each application. All of them are stored in a git repository at github³.

The application catalog is a JSON dictionary, where each application is described with the following fields:

- **app_name**: human readable application name, for showing it at user interfaces.
- **base_url**: download URL for the application.
- **file**: name of the file to be downloaded, relative to the **base_url**. Applications may be distributed as binaries or source files, the installer script handles each particular case.
- **dependencies**: list of applications (from the catalog) that need to be installed before this one.
- **installer**: name of the contextualization script that installs the application. The contents of this script depend on the characteristics of the application: it can install additional libraries at the Operating System level, compile (for applications distributed as source) or simply place binaries in the correct locations (for applications distributed as binaries).
- **versions**: dictionary containing the different available versions of the application. Inside this dictionary, there is an entry for each version where at least a **version_name** entry specifies a human readable name for the version. Optionally, it may include

³See <https://github.com/enolfc/feynapps> for details.

any of the fields in the application description, overriding the default values for the application.

The only mandatory fields are the `installer` and `versions`. A sample entry is shown below. The application name in this case is `FormCalc` and depends on the `FeynHiggs` application⁴. There are two different versions, 7.0.2 and 7.4, with the first one overriding the default value for the `base_url`:

```
"FormCalc": {
  "app_name": "FormCalc",
  "dependencies": [
    "FeynHiggs"
  ],
  "installer": "feyntools.sh",
  "base_url": "http://www.feynarts.de/formcalc/",
  "versions": {
    "7.0.2": {
      "base_url": "https://devel.ifca.es/~enol/feynapps/",
      "app_version": "7.0.2"
    },
    "7.4": {
      "app_version": "7.4"
    }
  }
}
```

The contextualizer exploits the user-supplied instance meta-data that is specified at the time of creation of the virtual machine. This is a free form text that is made available to the running instance through a fixed URL. In our case, the contextualizer expects to find a JSON dictionary with the applications to install on the machine. When the virtual machine is started, the contextualizer fetches the image meta-data and for each application listed in the JSON dictionary, it downloads the application from the specified URL in the catalog and executes the installation script. The script contents will depend on the application to install. It is executed as root user and can perform any required modifications in the system in order to properly setup the application (e.g. installation of additional libraries, creation of users, starting services, etc.). In most cases the script will extract the previously downloaded application archive and compile it with the virtual machine compiler and libraries. If the application has any dependencies listed in the catalog, the contextualizer will install them first, taking care of avoiding duplicated installations and cyclic dependencies.

The use of a git repository for managing the service provides complete tracking of the changes in the application catalog and the installation scripts, and allows researchers to add new applications or enhance the current installers by submitting pull requests to the repository. It also simplifies using always up-to-date versions of the tools and catalog at the virtual machines without having to recreate the virtual machine images by pulling the latest changes from the repository at instantiation time.

⁴ See Sect. 3.2 for more details on these codes.

To ease the use of the service, we have also extended the OpenStack dashboard to offer the contextualized instances from a web-based graphical interface. Fig. 2 shows this contextualization panel in horizon. The panel is a modified version of the instance launch panel, where a new tab includes the option to select which applications to install. The tab is created on the fly by reading the application catalog from a local copy of the git repository at the horizon machine—changes in the application catalog are made available with a periodic pull of the repository. For each selected application, the panel will include it in the instance meta-data, which will be used in turn by the contextualizer to invoke the scripts.

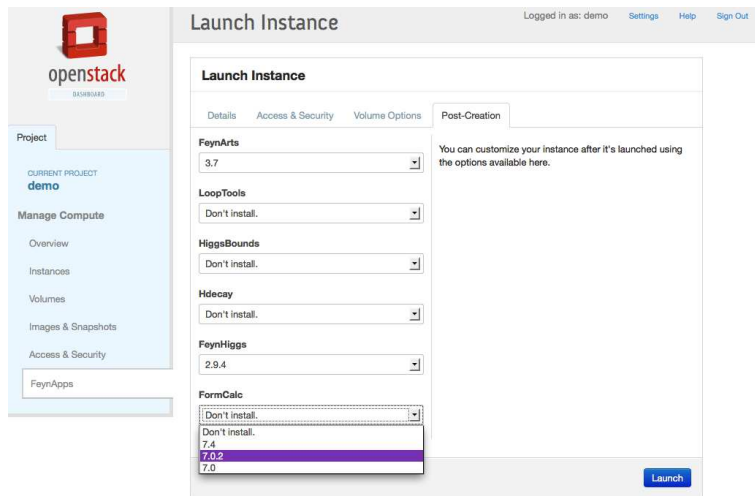


Figure 2: Image contextualization panel in Horizon. For each available application in the catalog, the user can select which version to install.

The panel restricts the images that can be instantiated to those that are ready to start the contextualization on the startup, which are identified in glance with the property `feynapps` set to `true`. This avoids errors due to selection of incorrect images and facilitates the addition of new images in the future without changing the dashboard.

3 Use Case: single processes on virtual machines

The first use case analyzed here concerns the evaluation of the decay properties of (hypothetical) elementary particles. The description of the underlying physics will be kept at a minimum; more details can be found in the respective literature.

3.1 The physics problem

Nearly all results of high-energy physics results are described with highest accuracy by the Standard Model (SM) of particle physics [8]. Within this theory it is possible to calculate the probabilities of elementary particle reactions. A more complicated theory that tries to go beyond the SM (to answer some questions the SM cannot properly address) is Supersymmetry (SUSY), where the most simple realization is the Minimal Supersymmetric Standard

Model (MSSM) [9]. Within this theory all particles of the SM possess “SUSY partner particles”. The physics problem used in our single-process example concerns the calculation of the desintegration probabilities of one of these SUSY partner particles, the so-called “heaviest neutralino”, which is denoted as $\tilde{\chi}_4^0$.

In the language of the MSSM the two desintegration modes investigated here are

$$\tilde{\chi}_4^0 \rightarrow \tilde{\chi}_1^0 h_1 , \quad (1)$$

$$\tilde{\chi}_4^0 \rightarrow \tilde{\chi}_1^+ W^- . \quad (2)$$

Here $\tilde{\chi}_1^0$ denotes the dark matter particle of the MSSM, h_1 is a Higgs boson, W^- is a SM particle responsible for nuclear decay, and $\tilde{\chi}_1^+$ is a corresponding SUSY partner. More details can be found in Ref. [10].

The evaluation is split into two parts. The first part consists of the derivation of analytical formulas that depend on the free parameters of the model. These parameters are the masses of the elementary particles as well as various coupling constants between them. These formulas are derived within `Mathematica` [11] and are subsequently translated into Fortran code; the second part consists of the evaluation of the Fortran code, see below. Numerical values are given to the free parameters (masses and couplings) and in this way the desintegration properties for (1), (2) are evaluated. In the case of (2) this includes also an additional numerical integration in four-dimensional space-time, which is performed by the Fortran code. However, no qualitative differences have been observed, and we will concentrate solely on process (1) in the following.

3.2 The computer codes and program flow

In the following we give a very brief description of the computer codes involved in our analysis. Details are not relevant for the comparison of the different implementations. However, it should be noted that the codes involved are standard tools in the world of high-energy physics phenomenology and can be regarded as representative cases, permitting a valid comparison of their implementation.

The first part of the evaluation is done within `Mathematica` [11] and consequently will be called “`Mathematica` part” in the following. It uses several programs developed for the evaluation of the phenomenology of the SM and MSSM. The corresponding codes are

- `FeynArts` [12]: this `Mathematica` based code constructs the “Feynman diagrams” and “amplitudes” that describe the particle decay processes (1) and (2). This code has been established as a standard tool in high-energy physics over the last two decades [12], as can be seen in the more than 600 use cases documented [13].
- `FormCalc` [14]: this `Mathematica` based code takes the “amplitudes” constructed by `FeynArts` and transforms them into analytical formulas in Fortran. For intermediate evaluations, `FormCalc` also requires the installation/use of `Form` [15], which is distributed as part of the `FormCalc` package. `FormCalc` is the standard tool to further evaluate `FeynArts` output, with more than 700 use cases documented [16].

- **LoopTools** [14]: this Fortran based code provides four-dimensional (space-time) integrals that are required for the evaluation of the decay properties. **FeynArts** and **FormCalc** *require* **LoopTools**, i.e. it can be seen as an integral part of the above described standard tool package.

Not all parameters contained in the analytical formulas are free, i.e. independent parameters. The structure of the SM and the MSSM fixes several of the parameters in terms of the others. At least one additional code is required to evaluate the dependent parameters in terms of the others,

- **FeynHiggs** [17]: this Fortran based code provides the predictions of the Higgs particles (such as h_1 in Eq. (1)) in the MSSM. The code has widely been used for experimental and theoretical MSSM Higgs analyses at LEP, the Tevatron and the LHC. For the latter it has been adopted as the standard tool for the MSSM Higgs predictions by the “LHC Higgs Cross Section Working Group” [19, 20].

The program flow of the **Mathematica** part is as follows. A steering code in **Mathematica** calls **FeynArts** and initiates the analytical evaluation of the decay properties of reaction (1) or (2). In the second step the steering code calls **FormCalc** for further evaluation. After the analytical result within **Mathematica** has been derived, **FormCalc** generates a Fortran code that allows for the numerical evaluation of the results. The code **LoopTools** is linked to this Fortran code. Similarly, also **FeynHiggs** is linked to this Fortran code. The creation of the Fortran code defines the end of the **Mathematica** part. The results of these analytical evaluations for the particle processes under investigations as well as for many similar cases (which used the same set of codes) have been verified to give reliable predictions [18].

The second part of the evaluation is based on Fortran and consequently will be denoted as “Fortran part” in the following. It consists of the execution of the Fortran code created in the **Mathematica** part. One parameter of the model is scanned in a certain interval, whereas all other parameters of the model are kept fixed. The calculation of the decay properties are performed for each value of the varied parameter. To be definite, in our numerical examples we have varied the complex phase of one of the free parameters, φ_{M_1} , between 0° and 360° in steps of one degree. In each of the 361 steps two parameter configurations are evaluated. Thus, in total the Fortran part performs 722 evaluations of the decay properties. As a physics side remark, the results are evaluated automatically in an approximate way (called “tree”) and in a more precise way (called “full”). The results of the Fortran part are written into an ASCII file. As an example of this calculation we show in Fig. 3 the results for the decay (1) for the two parameter configurations called S_g and S_h (both, “tree” and “full”) as a function of the parameter that is varied, φ_{M_1} . More details about the physics can be found in Ref. [10].

3.3 Performance analysis

We have measured the performance of the calculation of decay processes (1) and (2) in a virtualized environment.

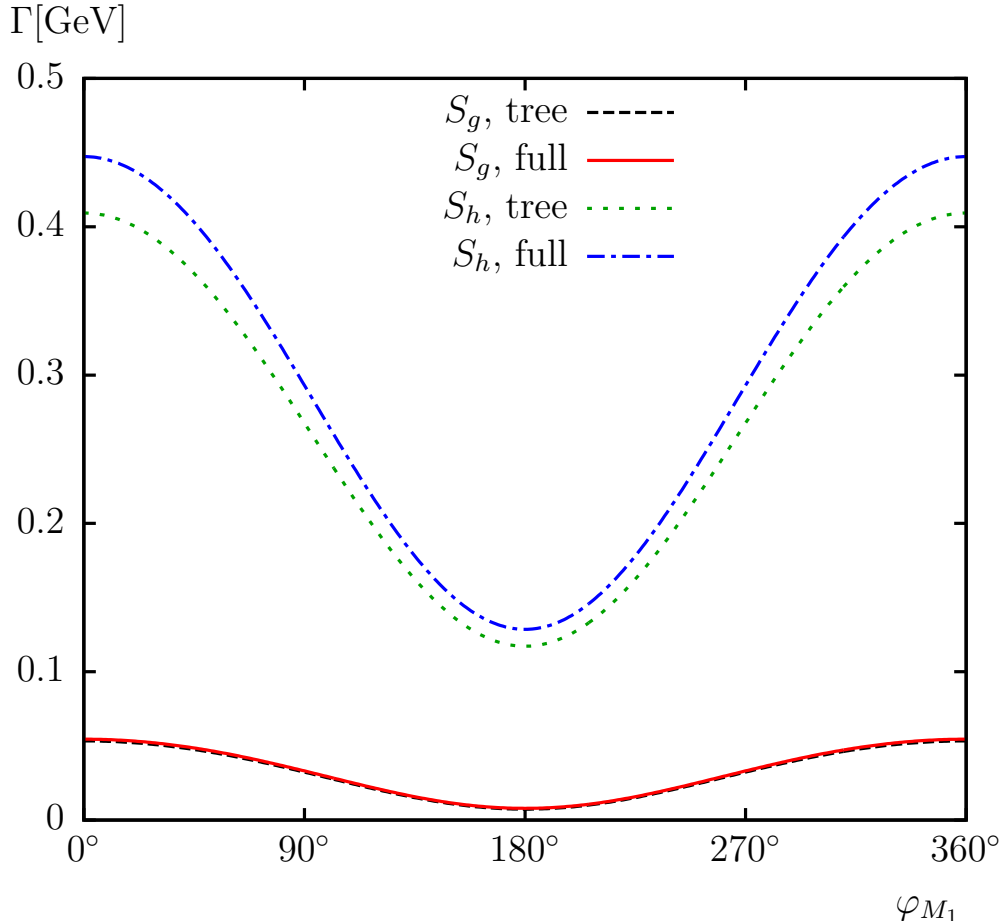


Figure 3: Example output of the evaluation of the properties of decay (1) for the two parameter configurations, S_g and S_h , in the approximation (“tree”) and the more precise way (“full”) as a function of φ_{M_1} [10]. The decay property Γ is given in its natural units “GeV” (Giga electron Volt).

Our set-up consisted on instantiating virtual machines as described in Sect. 2, including the necessary computational packages among them `Mathematica`, `FeynArts`, `FormCalc`, `FeynHiggs`, see above.

Since the nature of the codes is quite different, the computational time has been measured separately for the `Mathematica` part of the computation, and for the Fortran part of the code which involves basically Floating Point computing (i.e. without the load on file handling and input/output).

In order to fix our notation we introduce the following abbreviations:

- $S_{HT,nHT}(c)$ denotes a virtual machine consisting on c cores and 2GB of RAM.
- $M_{HT,nHT}(c)$ denotes a virtual machine consisting on c cores and 4GB of RAM.
- $L_{HT,nHT}(c)$ denotes a virtual machine consisting on c cores and 7GB of RAM.

- $XL_{HT,nHT}(c)$ denotes a virtual or physical machine with c cores and 14GB of RAM.

The subscripts HT and nHT refer to Hyperthreading enabled or disabled on the virtual machine, respectively. For instance, $M_{HT}(2)$ denotes a virtual machine with two physical cores, Hyperthreading enabled (i.e. 4 logical cores) and 4GB of RAM.

3.3.1 Single process on multicore virtual machines

In our first test we submit a single process to the system (regardless of how many cores are available). We plot in Fig. 4 the time that only the **Mathematica** part of the code takes, as a function of the configuration of the machine employed. Time measurements were taken using the GNU time command, that displays information about the resources used by a process as collected by the Operating System.

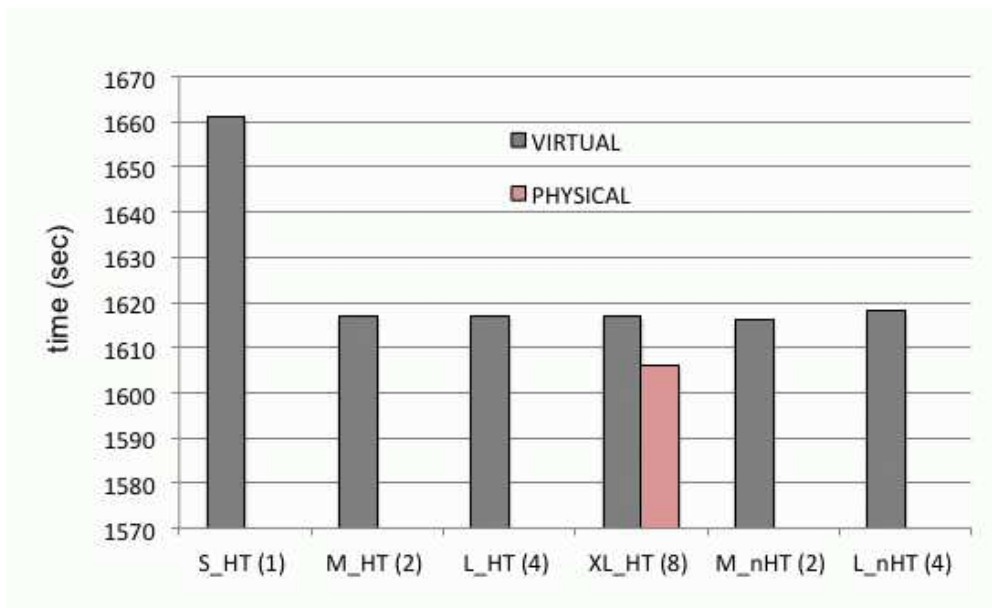


Figure 4: Execution time in seconds of the **Mathematica** part. One single process has been started on the different virtual machines configurations. The execution time on the equivalent physical machine has been included for comparison for $XL_{HT}(8)$. The corresponding detailed numbers can be found in Tabs. 1 – 3. The scale of the y-axis has been blown to make the differences visible to the eye.

As we see the **Mathematica** part is hardly affected by the size of the machine, once the virtual machine large enough. The effect observed with $S_{HT}(1)$ is an overhead due to the extra work that the only core needs to do to handle both, **Mathematica** and the guest Operating System. Hyperthreading is not enough to overcome the penalty in performance if only one core is used. However when more than one core is available one can see a constant performance regardless of the size of the virtual machine, and also regardless or whether Hyperthreading is enabled or not.

We have also included in this figure the comparison with the time it takes on the $XL_{HT}(8)$ machine without virtualization, what is called the “physical machine”. We see the physical

machine is only slightly faster, about a 1%. The degradation of performance in this case is therefore minimal. A more detailed comparison of virtual and physical machines can be found below.

Results turn out qualitatively different in the analysis of the Fortran part of the code, as can be seen in Fig. 5. This part is dominated by Floating Point calculations and few input/output or file handling, The first difference we see already at the smaller machines, where we do not observe anymore overheads due to the size of the virtual machine. The second difference to the *Mathematica* part of the code is that enabling the Hyperthreading does imply a penalty on performance on the order of a 4%. This is to be expected on general grounds due to the performance caveats induced by Hyperthreading on floating-point dominated applications, coming from the fact that the cores are not physical but logical, and the FPU unit is the same physical one for the two logical cores.

As for the comparison with the physical machine without virtualization, again shown for $XL_{HT}(8)$, we see that virtualization has degraded performance by about a 3% which is still a very small impact. Thus the influence of the host operating system is very small in low load situations.

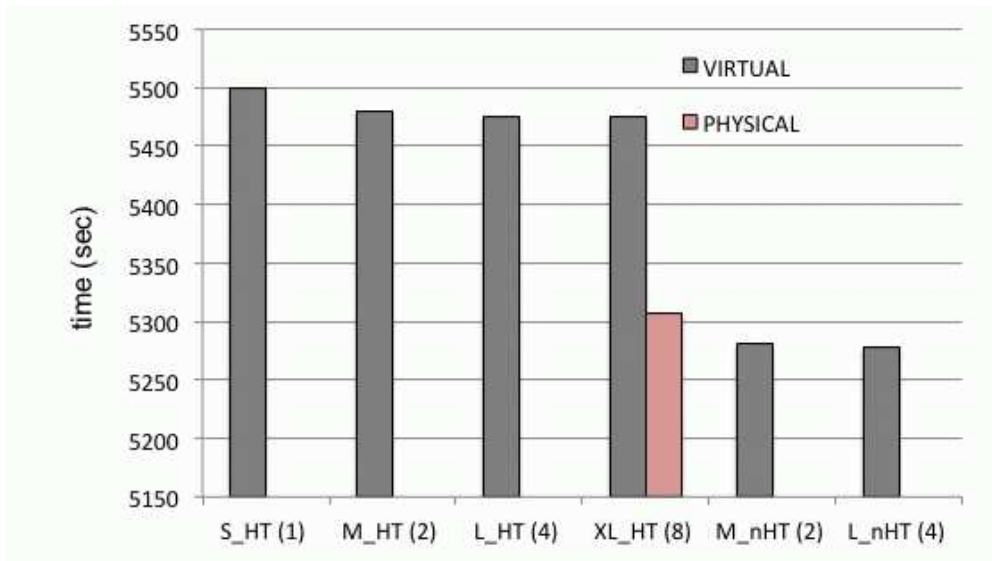


Figure 5: Execution time in seconds of the Fortran part. One single process has been started on the different virtual machines configurations. The execution time on the equivalent physical machine has been included for comparison for $XL_{HT}(8)$. The corresponding detailed numbers can be found in Tabs. 1 – 3. The scale of the y-axis has been blown to make the differences visible to the eye.

For both parts of the evaluation, the *Mathematica* part and the Fortran part, the percentage of system time employed during the computations is negligible. For the *Mathematica* dominated part of the computation it starts at 3% in $S_{HT}(1)$, to decrease down to a 1,5% in the rest of series. In the Fortran part it stays constant at about 0.2%.

3.3.2 Multiple simultaneous processes on multicore virtual machines

In this section we investigate the behavior of the performance in virtual machines under high load circumstances. For that we use a machine with 4 physical cores, Hyperthreading enabled, thus 8 logical cores.

To fix the notation we have adapted the previous definition as follows (in this test Hyperthreading is always enabled, therefore we drop the subscript for simplicity)

- $M(c/p)$ denotes a virtual machine consisting on c cores and 4GB of RAM and p concurrent processes running.
- $L(c/p)$ denotes a virtual machine consisting on c cores and 7GB of RAM and p concurrent processes running.
- $XL(c/p)$ denotes a virtual or physical machine with c cores and 14GB of RAM and p concurrent processes running.

The test was performed as follows. First we instantiate a virtual machine with a number of logical cores c . Then we start from $p = 1$ up to $p = c$ simultaneous processes in order to fill all the logical cores available, and measure how long each of the simultaneous processes takes to complete. Since not all the simultaneous processes take the same time to complete, we have taken the time of the slowest one for the plots. Conservatively speaking, this is the real time that the user would have to wait. The difference between the maximum and minimum times is not significative for our analysis (see Tabs. 4, 5 in Appendix B for more details on actual times).

In Fig. 6 we plot the execution time in seconds of the `Mathematica` part of the code for the M , L and XL machines with various number of processes as described above. In the XL case, for comparison, we also show the execution time in the physical machine. The first observation is that the degradation on the performance appears only when we load the system with more processes than the existing physical cores (i.e. more than 4). Thus we conclude that this is not an effect of virtualization, but rather of Hyperthreading. In the comparison of the virtual and the physical machines, shown for $XL(8/n)$ in Fig. 6, one can see that the virtualization does not really imply a penalty on the performance.

An interesting effect in this comparison can be observed when submitting $p = 6$ or more simultaneous processes. Against intuition the physical machine execution time is larger than the virtual machine execution time. This fact can only be explained if the virtualized operating system manages to handle better the threads than the normal operating system, which relies only Hyperthreading to distribute the system load.

To investigate this effect we plot in Fig. 7 the percentage of system time which the operating systems employed on the runs. We can see how at $XL(8/6)$ the physical machine does spend less sytem time than expected, and indeed, it is not managing the load of the 6 processes on the 8 logical cores in the most efficient way. In this case the spread in execution time between the fastest and the slowest processor is very large (2572 seconds versus 1899 seconds, where the latter is faster than the fastest time on the virtual machine, 2359 seconds), see Tabs. 4, 5 in Appendix B.

To conclude we plot in Fig. 8 the equivalent execution times in the Fortran dominated part of the calculation. We see that essentially the same pattern of behavior reproduces:

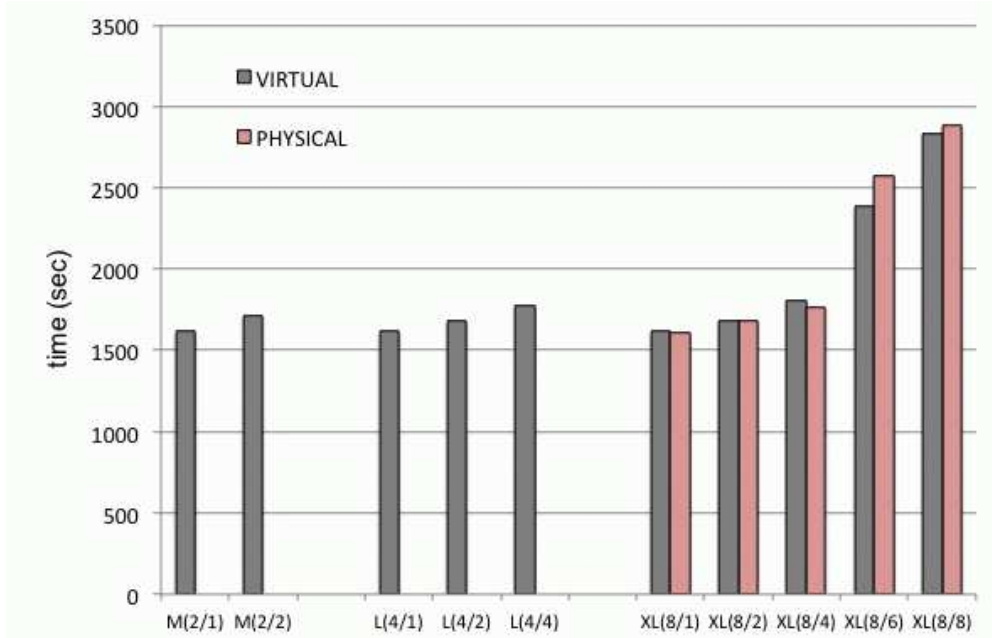


Figure 6: Execution time in seconds of the parts of the calculation involving Mathematica. The execution time on the equivalent physical machine has been included for comparison. The corresponding detailed numbers can be found in Tabs. 4, 5.

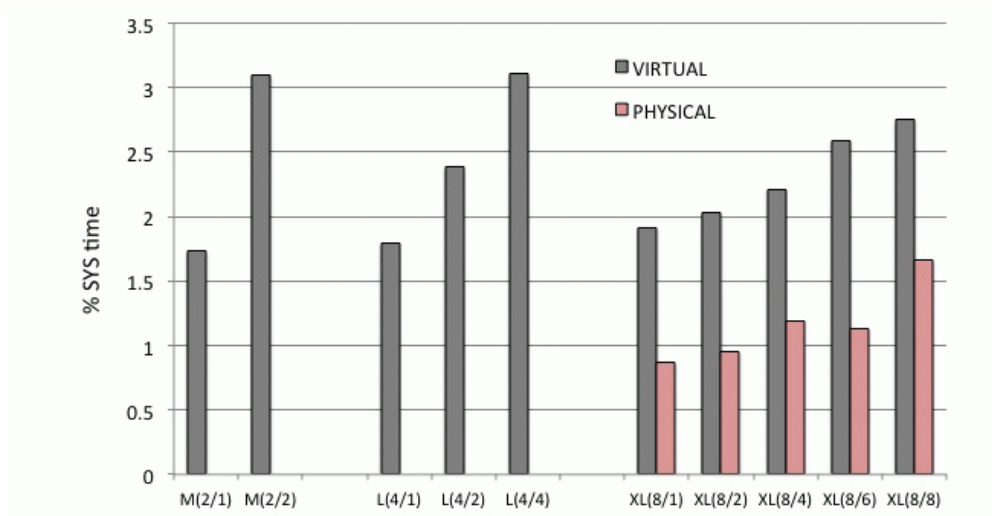


Figure 7: Percentage of system time employed by the virtual machine in the Mathematica part. The same percentage on the equivalent physical machine has been included for comparison in the *XL* case. The corresponding detailed numbers can be found in Tabs. 4, 5.

the load of the machines have a sizable effect on the execution time only for more than 4 simultaneous processes, and the virtual and physical machines show negligible differences.

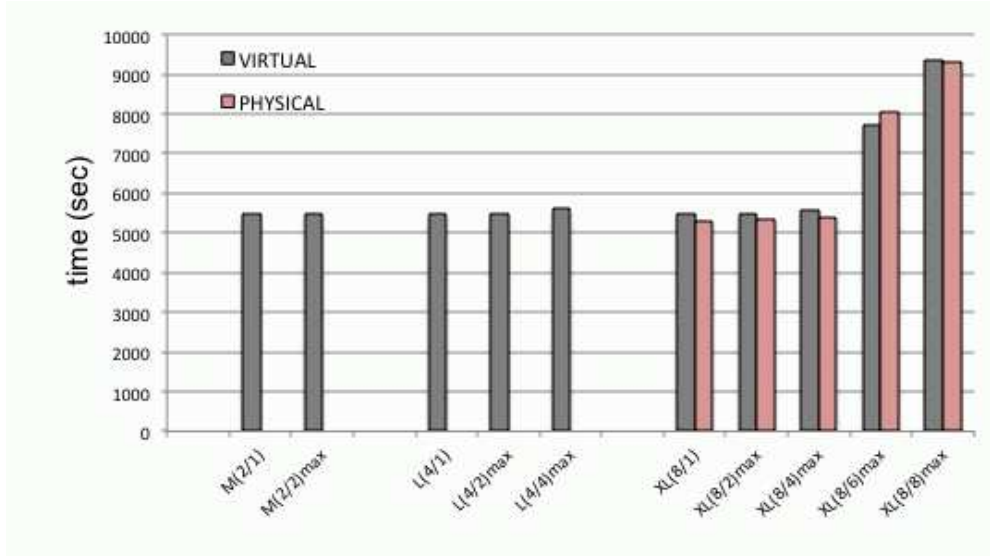


Figure 8: Execution time in seconds of the Fortran part. The execution time on the equivalent physical machine has been included for comparison for the *XL* case. The corresponding detailed numbers can be found in Tabs. 4, 5.

We also measured the memory consumption of the applications to ensure that swapping had no effects on the applications' execution. The *Mathematica* part memory footprint was collected using *Mathematica* memory management variable `MaxMemoryUsed[]`; while the Fortran part footprint was measured with the Valgrind [21] heap profiler tool. The maximum memory consumption for the *Mathematica* part was 691.1 MB. The Fortran part had a lower memory consumption with a maximum of 189.1 MB for the compilation of the resultant codes from *FormCalc* and 36.9 MB for the execution. These values are well below the minimum 1.75 GB of RAM per core (as in the *XL(8/n)* case) available in the virtual machines. The possibility of selecting the size of the virtual machine upon startup allows users to adapt their virtual infrastructure to the particular memory requirements of their applications.

4 Use Case: MPI Parallelization

The second use case analyzed here concerns a parameter scan as a typical application in the field of high-energy physics phenomenology. It also constitutes a perfect example that can be easily parallelized, see below for more details. For each point in the parameter scan an evaluation of Higgs boson properties that depend on this parameter choice is performed. As in the previous section, the description of the underlying physics will be kept at a minimum, and more details can be found in the respective literature.

4.1 The physics problem

Also this physics problem is taken from the MSSM. This model possesses several free parameters. Since they are unknown, a typical example of an analysis within this model requires extensive parameter scans, where the predictions for the LHC phenomenology change with the set of the scanned parameters.

After the discovery of a Higgs-like particle at the LHC [22, 23] the Higgs bosons of the MSSM are naturally of particular interest. The most relevant free parameters of the MSSM in this respect are

$$M_A \text{ and } \tan \beta . \tag{3}$$

M_A denotes the mass of a Higgs particle in the MSSM, β is a “mixing angle”, see Ref. [24] for further details.

A typical question for a choice of parameters is, whether this particular combination of parameters is experimentally allowed or forbidden. A parameter combination, in our case a combination of M_A and $\tan \beta$, can result in predictions for the Higgs particles that are in disagreement with experimental measurements. Such a parameter combination is called “experimentally excluded”. In the example we are using, two experimental results are considered. The first are the results from the LHC experiment itself. The other set are the results from a previous experiment, called “LEP” [25].

4.2 The computer codes and program flow

In the following we give a very brief description of the computer codes involved in this analysis. Details are not relevant for the comparison of the various levels of parallelization. As in the previous example, it should be noted that the codes involved constitute standard tools in the world of high-energy physics phenomenology and can be regarded as representative cases, permitting a valid comparison of their implementation.

The main code that performs the check of a Higgs prediction with results from the LHC and LEP is

- **HiggsBounds** [26]: this Fortran based code takes input for the model predictions from the user and compares it to the experimental results that are stored in the form of tables (which form part of the code). **HiggsBounds** has been established as the standard tool for the generic application of Higgs exclusion limits over the last years. It has been linked to many other high-energy physics standard codes to facilitate their evaluation [27].

The predictions for the Higgs phenomenology are obtained with the same code used in the previous section,

- **FeynHiggs** [17]: this Fortran based code provides the predictions of the Higgs particles in the MSSM (for more details see the previous section).

In our implementation a short steering code (also in Fortran) contains the initialization of the parameter scan: two loops over the scan parameters, M_A and $\tan\beta$, are performed in the ranges (omiting physical units),

$$\begin{aligned} M_A &= 90 \dots 500 , \\ \tan\beta &= 1.1 \dots 60 , \end{aligned} \tag{4}$$

with 120 steps in each parameter, resulting in 14400 scan points. As a physics side remark: the other free parameters are set to fixed values, in our case according to the m_h^{\max} scenario described in Ref. [24]. However, details are not relevant for our analysis.

The steering code calls the code **HiggsBounds**, handing over the scan parameters. Internally **HiggsBounds** is linked to **FeynHiggs**, again handing over the scan parameters. **FeynHiggs** performs the prediction of the Higgs phenomenology, and the results are given back to **HiggsBounds**. With these parameters the code can now evaluate whether this parameter combination is allowed or disallowed by existing experimental results. The corresponding results are stored in a simple ASCII file, where one file contains the points excluded by the LHC, another file the points excluded by LEP. As an example, we show in Fig. 9 the results for this scan in the two-dimensional M_A - $\tan\beta$ plane. Points marked in red, according to the evaluation with **HiggsBounds/FeynHiggs** are in disagreement with experimental results from the LHC, and blue points are in disagreement with experimental results from LEP. White points are in agreement with the currently available experimental results.

4.3 MPI parallelization

The parameter scan performed by the code is a typical example of an embarrassingly parallel computation, where each parameter evaluation can be computed independently of the others, without requiring any communication between them. This kind of problems can be easily parallelized by dividing the parameter space into sets and assign them to each available processor. An OpenMP [28] parallelization was discarded due to the use of non thread-safe libraries in the code, so we opted for using MPI [29] for developing the parallel version of the code.

In the parallel version, the steering code in Fortran was modified to have a single process that initializes the computation by setting the number of steps (by default 120 steps in each parameter) and values for the fixed free parameters and broadcasting all these values to the other processes in the computation. The parameter space is then divided equally among all processes, which perform the evaluation and write their partial results to independent files without any further communication between processes. Once the computation finishes, the partial results files are merged into a single file with all results. A master/worker parallelization with dynamic assignment of the parameters to each worker was not considered because the execution time per evaluation is almost constant hence there is no need to balance the work load between the workers.

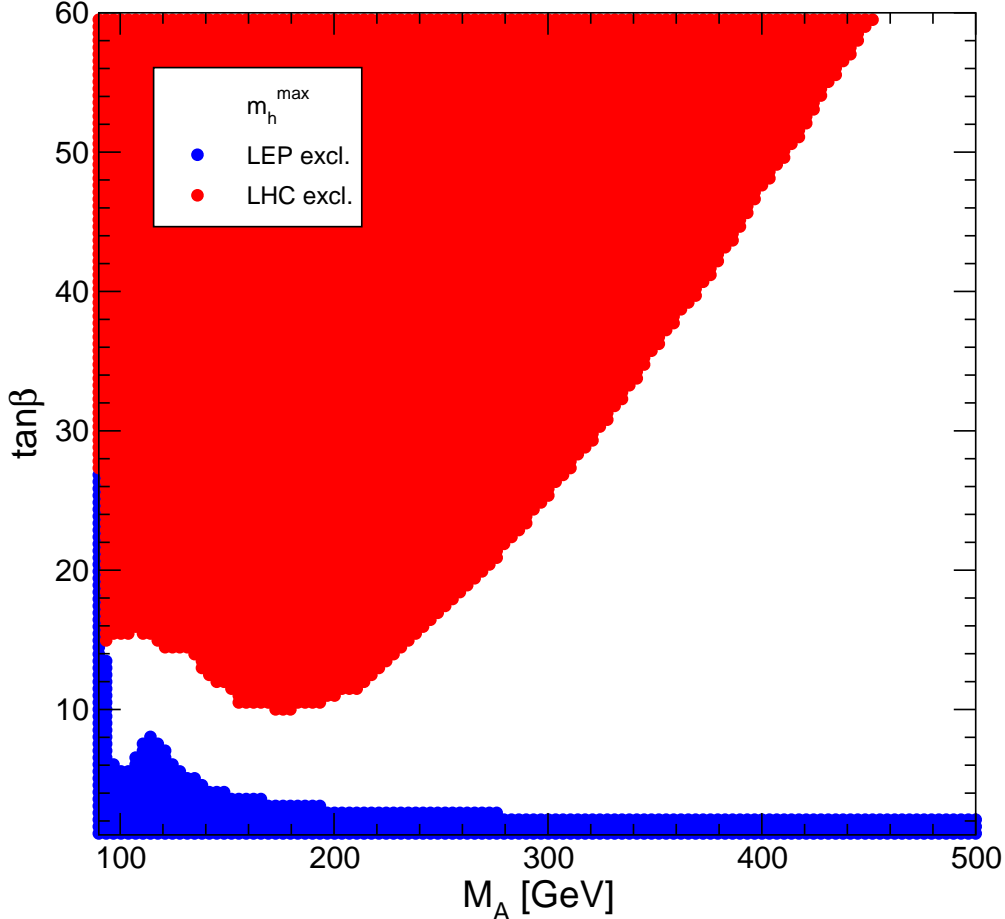


Figure 9: Example output of the MSSM scan in the two free parameters M_A and $\tan\beta$. The parameter M_A is given in its natural units “GeV” (Giga electron Volt).

4.4 Performance analysis

We have measured the scalability and performance of the two-dimensional M_A - $\tan\beta$ plane scan described in Section 4.2 with 14400 scan points in a virtualized environment. As in the previous case, we have instantiated the virtual machines using our contextualization mechanism to install `FeynHiggs` and `HiggsBounds` packages. The MPI code was compiled with `Open MPI v1.2.8` [30] as provided in the Operating System distribution.

These tests were performed on virtual machines that use the complete hardware, with and without Hyperthreading enabled (4 or 8 logical cores respectively) and the equivalent physical machine with the same number of cores and RAM to compare the performance without virtualization.

We plot in Fig. 10 the execution time for the parameter scan using from 1 (serial version) up to the number of cores available in each machine. The parallel versions time include also the final merge of the partial result files.

As we see the performance degradation due to virtualization is minimal, below 5% for all executions, and the difference in execution time with and without HyperThreading for

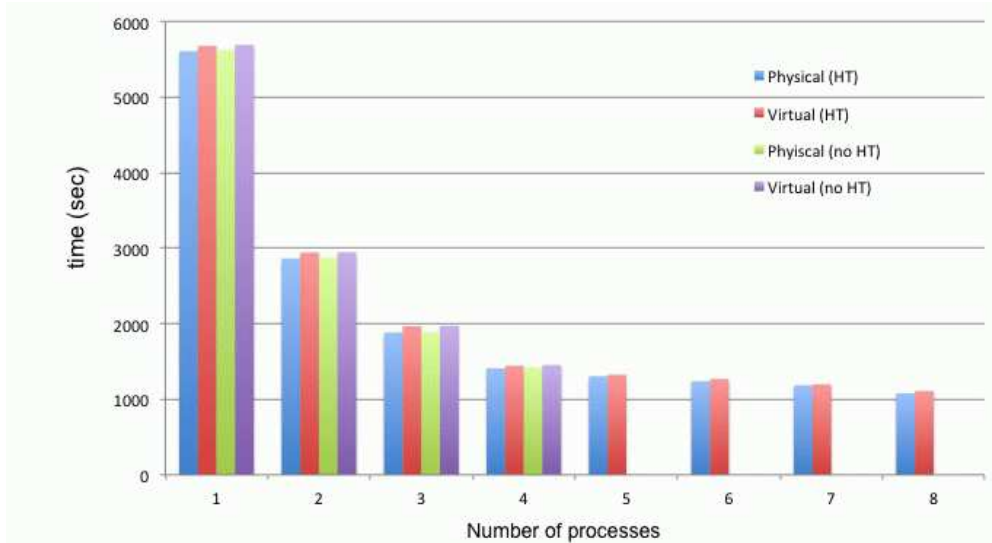


Figure 10: Execution time in seconds of the application for different number of processes, both in Virtual and Physical machines with and without HyperThreading.

the same number of processes is negligible. The difference between the virtual and physical machine decreases as the number of processes grows above 4. This effect, also seen in the case of multiple processes in Section 3, is due to the use different management the HyperThreading cores at the virtualized Operating System.

Since there is no communication overhead in the implementation, the application scales linearly with the number of processes given equally powerful CPUs. As seen in the plot, the scalability of the application is almost linear up to 4 processes (the same number of processes as available physical cores) and it flattens as the Operating System uses the logical cores provided by the HyperThreading.

5 Conclusions

We have described a new computing environment for particle physics phenomenology that can easily be translated to other branches of science. It is based on “virtual machines”, using the OpenStack infrastructure. In view of the performance, it is necessary to distinguish between two questions: the benefits that virtualization brings to researchers in terms on accesibility to computing resources, and the question of code performance and in general penalties due to the host operating system.

About the first question the setup of OpenStack and the development of the self-instantiation mechanism has been clearly appreciated by the researchers doing this type of computations. The solution removes many of the barriers described in the introduction of this article regarding complex code installation, machine availability, and automatization of workflows.

An additional benefit of this set-up is that OpenStack allows the user taking snapshots of the virtual machine, which are stored on a repository, and which the owner of the snapshot can instantiate again at any moment, recovering the session as they saved it. This is a very

practical feature because it allows researchers to “save” the current status on the virtual machine, and continue working at any other moment without blocking the hardware in the mean time.

The second question is performance. We have analyzed a set of representative codes in the area of particle physics phenomenology, so that our results can be extrapolated to similar codes in the area. The results are very positive, as no excessive penalty due to virtualization can be observed. At most we observe degradations in performance on the order of 3% for the parts of the codes dominated by Floating Point Calculations. For other calculations the degradation was even less. We have furthermore analyzed the influence of system time in the virtual machines. We found that the virtualization has no significant impact on the system time.

Evidently, the possibility of accessing resources in a more flexible way, the time that researchers spare using the new environment on software configuration compensates largely the usage of virtualized resources for the codes under investigation.

Acknowledgements

I.C. and E.F. thank the European Commission funding via EGI-InSPIRE Grant Contract number RI-261323, EMI Grant Contract number RI-261611 and FPA-2008-01732. The work of S.H. was partially supported by CICYT (grant FPA 2010-22163-C02-01). S.H. and F.v.d.P. were supported in part by the Spanish MICINN’s Consolider-Ingenio 2010 Programme under grant MultiDark CSD2009-00064 and the project “Computacion Avanzada en materiales y fenomenos de transporte” Grant number MEC-FIS-2009-12648-C03-02. G.B. would like to thank to the Portuguese Foundation for Science and Technology under the context of the Ciencia 2008 program jointly funded by the European Social Fund and by MCTES national funds - through POPH - NSRF-Type 4.2.

Appendix A: User access mechanisms

In this Appendix we describe the user access mechanisms that we have implemented.

A.I Authentication

Keystone performs the validation of user’s credentials (username/password) using a configurable back-end, which also stores all the data and associated meta-data about users, *tenants* (groups in OpenStack terminology) and roles associated to each user. There are four back-ends provided in the default OpenStack distribution: Key-Value Store (KVS), which provides an interface to other stores that can support primary key lookups (like a hash table); SQL, that stores data in a persistent database using SQLAlchemy; LDAP, that uses a LDAP server where users and tenants are stored in separate subtrees; and PAM, for simple mapping of local system users to OpenStack. The typical deployment uses the SQL backend.

Additional authentication mechanisms, e.g. those not based on username/password credentials, can be implemented using the Pluggable Authentication Handler (PAH) mechanism.

A pluggable authentication handler analyzes each user request and, if it's able to handle it, authenticates the user before the default back-end is executed.

Scientific computing and data centers provide services to scientific collaborations that often go beyond a single institution, creating federation of resources where users can access to the different providers using a single identity.

Grid infrastructures base the authentication and authorization of users on X.509 certificates and Virtual Organizations (VO). A Virtual Organization comprises a dynamic set of individuals (or institutions) defined around a set of resource-sharing rules and conditions. The current pan-european grid infrastructure use the Virtual Organization Management System (VOMS) for managing the users and resources within each VO. VOMS provides signed assertions regarding the attributes of a user belonging to a VO, thus enabling providers to trust these assertions and to define access rules to their resources based on the attributes. While a broad community of users are already familiarized with these authentication mechanisms, the use of X.509 certificates and proxies is considered to be one of the main barriers for new users and communities.

There are other mechanisms to provide identity federation across multiple providers that do not require the use of certificates, but these are poorly supported by the current scientific collaborations for accessing computing resources. LDAP can also be used to support federated authentication. LDAP is a well-known solution for authentication and it is widely used within the scientific data centers. However, the LDAP back-end included Openstack enforces a particular schema that does not fit most of existing deployments.

We have extended the authentication capabilities of Keystone with two new Pluggable Authentication Handlers, one supporting VOMS and another supporting LDAP authentication with arbitrary schema for storing user information. These modules enable the creation of a federated cloud infrastructure where users have a single identity across the different resource providers. The VOMS module enables the re-use of grid identity systems and leverages from existing experience of the resource providers, while the LDAP module enables the creation of simple federation without the inconvenience of the X.509 certificates for new users and communities.

A.II VOMS Authentication

The VOMS authentication module is implemented as a Pluggable Authentication Handler in Keystone and executed as a WSGI [31] of an httpd server enabled to use OpenSSL and configured to accept proxy certificates (VOMS assertions are included in proxy certificates). Fig. 11 shows the call sequence for the authentication and authorization of a user using VOMS.

Prior to the authentication, the user creates a proxy by contacting the VOMS server. This proxy includes the distinguished name (DN) of the user and a set of attributes related to the VO (group and roles associated with the user). The authentication in Keystone is performed by requesting a token to the server, if successful, Keystone will return a token which is used for any subsequent calls to the other OpenStack services. In our implementation, the user authenticates against the httpd server with the VOMS proxy, and the server, after validation, includes the SSL information in the request environment. This information reaches the VOMS module that will authorize the request checking if the proxy is valid and if the VO

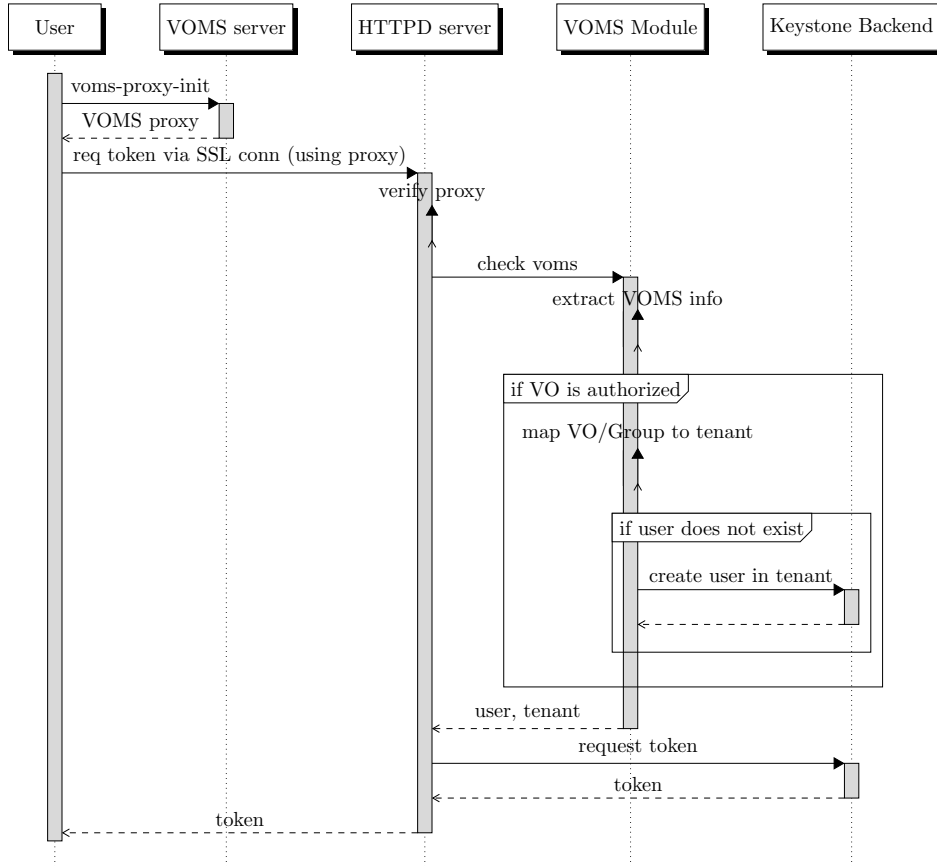


Figure 11: VOMS Authentication sequence diagram.

is allowed in the server.

Once the proxy is considered valid and allowed, the module maps VO attributes included in the proxy to a local OpenStack tenant using a configuration file. The user DN in the proxy is used as user name in Keystone. The mapped local tenant must exist in advance for a user to be authenticated. The VOMS module can automatically create the user in Keystone if enabled in configuration. This allows to easily establish access policies based only in the membership to a given VO, instead of giving access to individuals. Once a user has been granted access, the administrator can manage it as with any other user in the Keystone back-end (i.e. disable/enable, grant/revoke roles, etc.).

A.III LDAP Authentication

The LDAP authentication modules takes profit from the authentication features of the apache httpd server. In this case the authentication phase is delegated to the server which can authenticate users against LDAP with arbitrary schemas. This way, we use a reliable and tested code that is used in production systems and is actively maintained by the apache developers. Moreover, we avoid the introduction of security risks by minimizing the code the deals with the authentication. Once the server has authenticated the request, it will pass

the user name through the environment of the WSGI module.

The LDAP module uses a configuration file that specifies using regular expressions which users are allowed and to what tenants they should be mapped in the system. If the user is authorized, the user can be created automatically in Keystone as in the VOMS case. Finally, the token is returned to the user. Figure 12 shows the sequence diagram for this process.

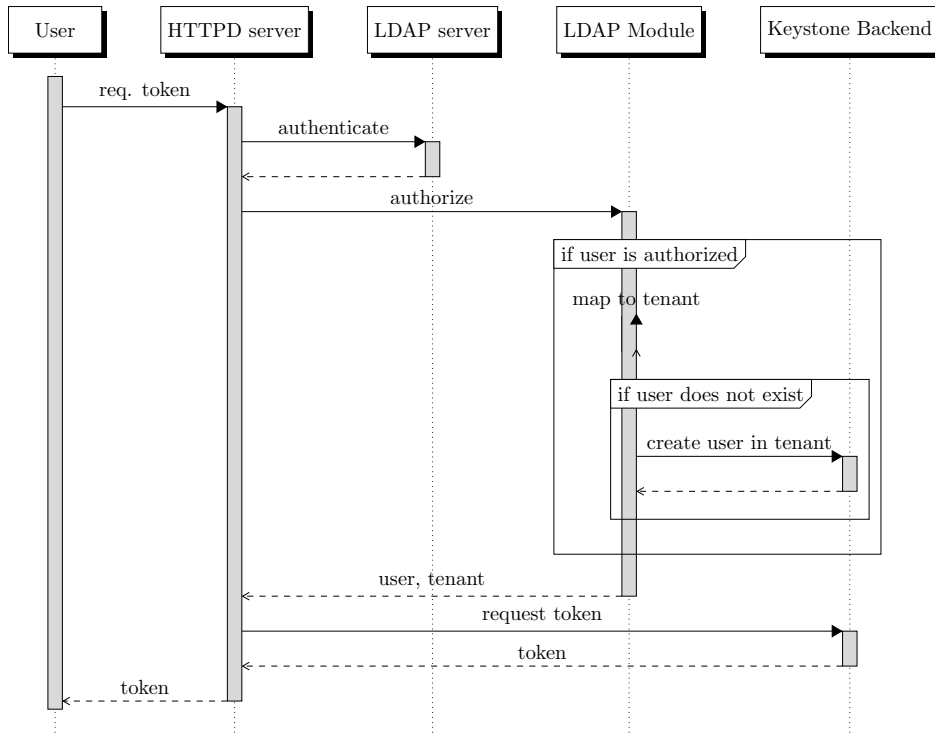


Figure 12: LDAP Authentication sequence diagram.

Appendix B: Detailed computation times

In this Appendix we give detailed numbers on the execution times of the analysis in Sect. 3. The notations are the same as in that section.

machine (cores)	Math			Fortran			Total		
	real	user	sys	real	user	sys	real	user	sys
$S_{HT}(1)$	1661.06	1601.87	48.38	5500.06	5466.54	11.07	7161.24	7068.43	59.47
$M_{HT}(2)$	1617.06	1613.56	28.37	5480.03	5465.36	12.20	7097.20	7078.99	40.58
$L_{HT}(4)$	1617.05	1615.18	29.38	5475.64	5461.08	12.28	7092.80	7076.33	41.68
$XL_{HT}(8)$	1617.19	1615.86	31.00	5475.95	5461.20	12.48	7093.25	7077.12	43.50

Table 1: Computation time (sec) of virtual machines with hyperthreading (HT), divided in **Mathematica** part, Fortran part, and total time. Computation time is divided in real, user, sys, denoting respectively real time, processor time for computation, and system time.

machine (cores)	Math			Fortran		
	real	user	sys	real	user	sys
$M_{nHT}(2)$	1616.78	1613.12	28.20	5281.21	5266.46	11.69
$L_{nHT}(4)$	1618.9	1613.9	33.8	5278.9	5264.0	12.6

Table 2: Computation time (sec) of virtual machines without hyperthreading (nHT).

machine (cores)	Math			Fortran		
	real	user	sys	real	user	sys
$R_{HT}(8)$	1605.1	1584.8	13.9	5306.9	5290.8	6.6

Table 3: Computation time (sec) of physical machine R with hyperthreading (HT).

machine (cores/proc.)	Math			Fortran		
	real	user	sys	real	user	sys
$M_{HT}(2/1)$	1617.1	1613.6	28.4	5480.0	5465.4	12.2
$M_{HT}(2/2)$ max	1708.9	1647.2	52.6	5500.7	5472.7	12.2
$M_{HT}(2/2)$ min	1713.4	1650.6	53.4	5493.6	5469.7	12.2
$L_{HT}(4/1)$	1617.1	1615.2	29.4	5475.6	5461.1	12.3
$L_{HT}(4/2)$ max	1678.6	1653.2	39.5	5488.0	5473.3	12.4
$L_{HT}(4/2)$ min	1672.4	1656.4	36.1	5491.0	5476.0	12.6
$L_{HT}(4/4)$ max	1771.1	1709.0	54.5	5602.4	5580.7	12.3
$L_{HT}(4/4)$ min	1775.3	1711.8	53.8	5511.9	5489.8	12.7
$XL_{HT}(8/1)$	1617.2	1615.9	31.0	5476.0	5461.2	12.5
$XL_{HT}(8/2)$ max	1678.4	1671.2	34.4	5492.4	5477.1	13.1
$XL_{HT}(8/2)$ min	1676.8	1668.6	35.3	5493.4	5478.2	13.0
$XL_{HT}(8/4)$ max	1807.0	1790.9	39.7	5566.1	5549.4	13.9
$XL_{HT}(8/4)$ min	1809.6	1786.3	45.1	5521.6	5504.8	14.0
$XL_{HT}(8/6)$ max	2385.7	2333.8	62.8	7706.1	7684.6	17.2
$XL_{HT}(8/6)$ min	2358.8	2306.8	63.0	7558.8	7535.5	17.2
$XL_{HT}(8/8)$ max	2835.5	2741.8	78.2	9375.0	9344.9	18.7
$XL_{HT}(8/8)$ min	2818.9	2728.8	77.5	9329.9	9295.4	18.6

Table 4: Computation time (sec) of virtual machine with multiple equal processes.

machine (cores/proc.)	Math			Fortran		
	real	user	sys	real	user	sys
$R_{HT}(8/1)$	1605.1	1584.8	13.9	5306.9	5290.8	6.6
$R_{HT}(8/2)$ max	1683.7	1642.9	15.7	5345.4	5329.3	6.5
$R_{HT}(8/2)$ min	1686.9	1646.2	17.1	5311.7	5295.5	6.6
$R_{HT}(8/4)$ max	1763.4	1696.1	20.6	5401.6	5384.9	6.9
$R_{HT}(8/4)$ min	1765.6	1700.4	19.9	5317.6	5301.0	6.9
$R_{HT}(8/6)$ max	2572.4	2449.5	29.4	8063.2	8039.8	8.5
$R_{HT}(8/6)$ min	1899.1	1804.9	23.4	7060.7	7039.5	8.0
$R_{HT}(8/8)$ max	2882.7	2707.6	48.8	9320.7	9288.5	10.0
$R_{HT}(8/8)$ min	2862.3	2685.2	47.7	9291.8	9261.2	9.6

Table 5: Computation time (sec) of physical machine R with HT with multiple equal processes.

References

- [1] P. Mell and T. Grance, *NIST Special Publication* **800-145** (2011).
- [2] S. Brewer et al., *Lecture Notes in Computing Science* **7616** (2012) 849.
- [3] R. Alfieri et al., *Future Generation Computer Systems* **21(4)** (2005) 549.
- [4] See <http://www.opennebula.org> for details.
- [5] See <http://www.openstack.org> for details.
- [6] P. Barham, B. Dragovic, K. Fraser, S. Hand, T. Harris, A. Ho, R. Neugebauer, I. Pratt, and A. Warfield. *SIGOPS Oper. Syst. Rev* **37, 5** (2003) 164
- [7] J. Blomer, P. Buncic and R. Meuse. The CernVM File System (2013)
- [8] L. Glashow, *Nucl. Phys.* **22**, 579 (1961);
S. Weinberg, *Phys. Rev. Lett.* **19**, 1264 (1967);
A. Salam, J.C. Ward, *Phys. Lett.* **13** (1964) 168.
- [9] H. Nilles, *Phys. Rept.* **110** (1984) 1;
H. Haber and G. Kane, *Phys. Rept.* **117** (1985) 75;
R. Barbieri, *Riv. Nuovo Cim.* **11** (1988) 1.
- [10] A. Bharucha, S. Heinemeyer, F. von der Pahlen and C. Schappacher, *Phys. Rev. D* **86** (2012) 075023 [arXiv:1208.4106 [hep-ph]].
- [11] S. Wolfram, *The Mathematica Book*, Wolfram Media/Cambridge University Press, 1996.
- [12] J. Küblbeck, M. Böhm and A. Denner, *Comput. Phys. Commun.* **60** (1990) 165;
T. Hahn, *Comput. Phys. Commun.* **140** (2001) 418 [arXiv:hep-ph/0012260];
T. Hahn and C. Schappacher, *Comput. Phys. Commun.* **143** (2002) 54 [arXiv:hep-ph/0105349].
The program, the user's guide and the MSSM model files are available via <http://www.feynarts.de> .
- [13] See: <http://inspirehep.net/search?ln=en&p=refersto%3Arecid%3A539011> .
- [14] T. Hahn and M. Pérez-Victoria, *Comput. Phys. Commun.* **118** (1999) 153 [arXiv:hep-ph/9807565].
- [15] J. Vermaseren, *Symbolic Manipulation with FORM*, (Computer Algebra Netherlands, Amsterdam, 1991).
- [16] See: <http://inspirehep.net/search?ln=en&p=refersto%3Arecid%3A474106> .

- [17] S. Heinemeyer, W. Hollik and G. Weiglein, *Comput. Phys. Commun.* **124** (2000) 76 [arXiv:hep-ph/9812320]; *Eur. Phys. J. C* **9** (1999) 343 [arXiv:hep-ph/9812472]; G. Degrandi, S. Heinemeyer, W. Hollik, P. Slavich and G. Weiglein, *Eur. Phys. J. C* **28** (2003) 133 [arXiv:hep-ph/0212020]; M. Frank, T. Hahn, S. Heinemeyer, W. Hollik, R. Rzehak and G. Weiglein, *JHEP* **0702** (2007) 047 [arXiv:hep-ph/0611326]; T. Hahn, S. Heinemeyer, W. Hollik, H. Rzehak and G. Weiglein, *Comput. Phys. Commun.* **180** (2009) 1426; see <http://www.feynhiggs.de>.
- [18] S. Heinemeyer, H. Rzehak and C. Schappacher, *Phys. Rev. D* **82** (2010) 075010 [arXiv:1007.0689 [hep-ph]]; T. Fritzsche, S. Heinemeyer, H. Rzehak and C. Schappacher, *Phys. Rev. D* **82** (2010) 075010 [arXiv:1111.7289 [hep-ph]]; S. Heinemeyer, F. von der Pahlen and C. Schappacher, *Eur. Phys. J. C* **72** (2012) 1892 [arXiv:1112.0760 [hep-ph]]; S. Heinemeyer and C. Schappacher, *Eur. Phys. J. C* **72** (2012) 1905 [arXiv:1112.2830 [hep-ph]]; *Eur. Phys. J. C* **72** (2012) 2136 [arXiv:1204.4001 [hep-ph]].
- [19] See: <https://twiki.cern.ch/twiki/bin/view/LHCPhysics/CrossSections> .
- [20] See: <https://twiki.cern.ch/twiki/bin/view/LHCPhysics/MSSM> .
- [21] N. Nethercote and J. Seward, *Proceedings of ACM SIGPLAN 2007 Conference on Programming Language Design and Implementation* (2007).
- [22] G. Aad et al. [ATLAS Collaboration], *Phys. Lett. B* **716** (2012) 1 [arXiv:1207.7214 [hep-ex]].
- [23] S. Chatrchyan et al. [CMS Collaboration], *Phys. Lett. B* **716** (2012) 30 [arXiv:1207.7235 [hep-ex]].
- [24] M. Carena, S. Heinemeyer, C. Wagner and G. Weiglein, *Eur. Phys. J. C* **26** (2003) 601 [arXiv:hep-ph/0202167].
- [25] [LEP Higgs working group], *Phys. Lett. B* **565** (2003) 61 [arXiv:hep-ex/0306033]; *Eur. Phys. J. C* **47** (2006) 547 [arXiv:hep-ex/0602042].
- [26] P. Bechtle, O. Brein, S. Heinemeyer, G. Weiglein and K. Williams, *Comput. Phys. Commun* **181** (2010) 138 [arXiv:0811.4169 [hep-ph]]; *ibid.* **182** (2011) 2605 [arXiv:1102.1898 [hep-ph]]; see: <http://higgsbounds.hepforge.org/> .
- [27] See: <http://inspirehep.net/search?ln=en&p=refersto%3Arecid%3A803530> .
- [28] L. Dagum and R. Menon, *Comp. Sci. & Eng.* **5-1** (1998) 46.
- [29] [Message Passing Interface Forum] MPI-v2.2 (2009).
- [30] E. Gabriel et al., *Proceedings 11th European PVM/MPI Users' Group Meeting* (2004).
- [31] P. Eby, PEP-3333 (2010).